Title
SOA Formation Potential of Emissions from Soil and Leaf Litter

Journal
Environmental Science and Technology, 48(2)

ISSN
0013-936X

Authors
Faiola, Celia L
VanderSchelden, Graham S
Wen, Miao
et al.

Publication Date
2014-01-21

DOI
10.1021/es4040045

Environmental Science & Technology

Article

pubs.acs.org/est

SOA Formation Potential of Emissions from Soil and Leaf Litter

Celia L. Faiola,[†] Graham S. VanderSchelden,[†] Miao Wen,[†] Farah C. Elloy,[‡] Douglas R. Cobos,[§] Richard J. Watts,[‡] B. Thomas Jobson,[†] and Timothy M. VanReken[†,*]

[†]Laboratory for Atmospheric Research, Department of Civil & Environmental Engineering, Washington State University, Pullman, Washington 99164

[‡]Department of Civil & Environmental Engineering, Washington State University, Pullman, Washington 99164

[§]Decagon Devices, Inc., Pullman, Washington 99163

Supporting Information

ABSTRACT: Soil and leaf litter are significant global sources of small oxidized volatile organic compounds, VOCs (e.g., methanol and acetaldehyde). They may also be significant sources of larger VOCs that could act as precursors to secondary organic aerosol (SOA) formation. To investigate this, soil and leaf litter samples were collected from the University of Idaho Experimental Forest and transported to the laboratory. There, the VOC emissions were characterized and used to drive SOA formation via dark, ozone-initiated reactions. Monoterpenes dominated the emission profile with emission rates as high as 228 μg-C m^{-2} h^{-1}. The composition of the SOA produced was similar to biogenic SOA formed from oxidation of ponderosa pine emissions and α-pinene. Measured soil and litter monoterpene emission rates were compared with modeled canopy emissions. Results suggest surface soil and litter monoterpene emissions could range from 12 to 136% of canopy emissions in spring and fall. Thus, emissions from leaf litter may potentially extend the biogenic emissions season, contributing to significant organic aerosol formation in the spring and fall when reduced solar radiation and temperatures reduce emissions from living vegetation.

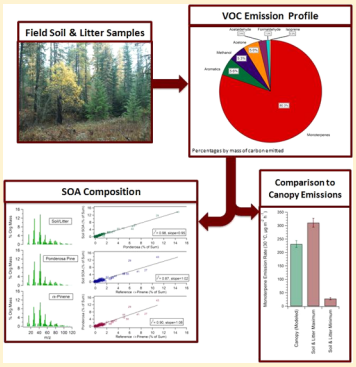

INTRODUCTION

Organic material comprises a major portion of atmospheric particulate mass loadings in a wide range of environments around the world.[1,2] The presence of organics within atmospheric particles impacts climate by changing the aerosol radiative properties—both directly by impacting light scattering and absorption and indirectly by altering hygroscopicity and thus cloud-forming potential.[3,4] Consequently, accurate modeling of the organic aerosol component is crucial to properly assess the climate change impacts of the total atmospheric aerosol, one of the least understood of all climate change radiative forcers.[5]

Among the many components contributing to the total atmospheric aerosol, secondary organic aerosol (SOA) is the most difficult to predict. State-of-the-art modeling techniques rarely match measured atmospheric SOA loadings, regardless of location, time, or scale.[6−9] This is largely due to the complex formation processes associated with SOA production. SOA is formed in the atmosphere from the oxidation of volatile organic compounds (VOCs), either in the gas or aqueous phase, to form less volatile products.[10,11] The chemistry can be affected strongly by local meteorological conditions or the presence of anthropogenic pollution.[12,13] Modeling SOA formation requires reliable estimates of both the emissions of the precursor organic vapors and a robust understanding of the chemical processing of those vapors upon entering the atmosphere. The most prevalent SOA precursors on a global scale are terpenoid compounds emitted from vegetation.[14] Much effort has gone toward developing parametrizations of VOC emissions from vegetation sources, such as those contained in the model of emissions of gases and aerosols from nature (MEGAN).[15,16]

While not considered a major global source of terpenoid emissions, soil and leaf litter still contribute significantly to VOCs in the atmosphere, particularly in spring and fall.[17,18] The research focus for soil and litter emissions has been primarily on methanol, acetone, acetaldehyde, and other VOCs with photoproducts that are too volatile to contribute significantly to SOA production. However, Isidorov and colleagues[19,20] examined the emissions more broadly and identified more than 100 organic compounds emitted from leaf litter, including many potential SOA precursors. Even so, the potential of soil and leaf litter as sources of SOA precursor emissions has generally been ignored due to results suggesting that their terpenoid emissions were insignificant relative to the emissions from trees, at least during summertime.[21−24]

Other research has indicated that in spring and fall, soil and leaf litter emissions may contribute more significantly to SOA formation in forest ecosystems. Mäkelä et al.[25] and Bigg[26] each linked the high rate of particle formation events observed in spring in a boreal forest in southern Finland to soil and leaf litter emission activity. Litter emissions of the dominant SOA

Received: September 8, 2013
Revised: November 27, 2013
Accepted: December 13, 2013
Published: December 13, 2013

precursors, terpenoids, have been shown to peak in late spring/early summer and autumn.[26−28] Laboratory measurements demonstrate that these terpenoid emissions can remain elevated throughout the early stages of leaf litter decomposition, up to 165 days, during which monoterpene emissions can approach or even exceed those from living vegetation.[28] In fact, one set of field measurements made in spring showed monoterpene emissions exceeding the contribution from living vegetation with values greater than 300 μg m^{-2} h^{-1}.[29]

Motivated by these findings, we present here the results of a recent study examining VOC emissions of soil and leaf litter collected from a temperate coniferous forest in northern Idaho in the United States. We characterize the amount and type of the VOC emissions as well as their SOA formation potential. This was accomplished by continuously monitoring VOC emissions from soil and litter samples in the laboratory, and performing aerosol growth experiments using those emissions as the SOA precursor source. Our results demonstrate that soil and leaf litter emissions of SOA precursors can be substantial, and may indeed represent a significant source under conditions typical of early spring and late autumn when foliar emissions from vegetation are low. This process could effectively extend the season for biogenic SOA formation within the forest ecosystem beyond the summertime period when emissions from living vegetation are dominant. Currently, models are not accounting for this potentially important emission source relevant to SOA formation.

EXPERIMENTAL SECTION

Sample Collection and Site Characterization. Soil and leaf litter samples were collected from the Big Meadow Creek site at the University of Idaho Experimental Forest on November 2, 2012 and November 9, 2012 (46.78432 N and 116.7948 W, 860 m above sea level). This temperate coniferous forest is dominated by ponderosa pine (*Pinus ponderosa*), Douglas fir (*Pseudotsuga menziesii*), western white pine (*Pinus monticola*), and western larch (*Larix occidentalis*). On each sampling day, five separate 30.5 × 40.5 × 9.0 cm^3 aluminum pans were filled with soil with leaf litter laid over the top. Litter depth varied between 4.0 and 10.5 cm. Prior to digging the soil, the leaf litter was carefully removed from the ground and placed in a separate pan. This procedure was used to maintain the integrity of the leaf litter and to minimize litter loss during soil sampling. Soil samples were then removed from the ground as intact units to preserve native structure and density, and transferred to the aluminum pan where the leaf litter was replaced by evenly distributing it over the top of the soil in the pan. Samples were immediately transported back to the laboratory in the aluminum pans and placed in the dynamic soil enclosure. All samples were collected within approximately a 15 m radius of one another. Bulk soil and litter samples were also collected on November 2 to characterize the substrate organic carbon at the sampling site. The soil and litter samples were oven-dried for 48 h at 55 and 80 °C, respectively, and ground to pass through a 0.5 mm sieve. Organic carbon content in each 0.1 g soil sample and 0.01 g leaf litter sample were determined using the Walkley-Black method.[30] The soil organic carbon content was 69.6 g/kg ±0.1% based on a triplicate analysis of two separate bulk soil samples. The litter organic carbon content was 572 g/kg ±0.6% based on triplicate analysis of a single bulk litter sample (values given are the mean ± the relative standard deviation).

The soil at The Big Meadow Creek site was characterized as silt loam based on the National Resource Conservation Service web soil survey.[31] Soil temperature, soil moisture, and leaf litter moisture were measured at five separate locations within the sampling plot on each sampling day (Decagon Devices model RT-1 soil temperature sensor and model GS3 soil moisture sensor). Soil temperature, soil moisture, and leaf litter moisture were 8.5 ± 0.4 °C, 0.313 ± 0.127 m^3 m^{-3}, and 0.216 ± 0.066 m^3 m^{-3}, respectively, on the first sample collection day and 1.9 ± 2.4 °C, 0.304 ± 0.067 m^3 m^{-3}, and 0.218 ± 0.071 m^3 m^{-3}, respectively, on the second sample collection day. Recent precipitation events were evident at the site during sample collection on both days. It had rained the night of November 1, 2012 and snowed lightly the evening of November 8, 2012.

Laboratory Chambers and Instrumentation. A dual chamber system was used to generate SOA from the VOC emissions of soil and leaf litter samples (Supporting Information, SI, Figure S1). Both chambers were composed of fluorinated ethylene propylene (Teflon FEP) material. One chamber was used to house the soil and leaf litter samples and will be referred to here as the dynamic soil emissions chamber. The other chamber was used to oxidize those emissions to form SOA and will be referred to as the aerosol growth chamber. The 0.9 × 0.9 × 0.9 m^3 soil emissions chamber accommodated five soil and leaf litter samples. Photosynthetically Active Radiation (PAR) was continuously monitored with an Apogee model SQ-215 quantum sensor. Temperature and relative humidity were continuously monitored with a Vaisala model HMP110 humidity and temperature probe. Soil temperature and moisture were monitored with a Decagon model GS3 soil moisture sensor. The soil emissions chamber was equipped with a high PAR output light (Lumatek High-Par Output HPS Lamp, 600W) set on a 12-h on/off cycle to simulate the day/night cycle. The soil emissions chamber was continuously purged with zero air at 9.5 standard L min^{-1} (Aadco model 737 pure air generator).

VOC emissions were monitored by sampling from the soil emissions chamber with an online gas chromatograph coupled to a mass spectrometer and flame ionization detector (Agilent model 6890/5973 GC-MS-FID, model DB-5 ms column) and a proton transfer reaction mass spectrometer (PTR-MS). The PTR-MS measurement method is described in detail elsewhere.[32] Briefly, mass scans from m/z 21 to m/z 210 were performed at 80 Td, as described in Jobson and McCoskey[33] with a cycle time of approximately 6 min. All VOC sampling lines were heated to 80 °C to minimize losses. The PTR-MS response was calibrated using a multicomponent compressed gas standard (Scott-Marrin) containing α-pinene, methanol, acetone, acetaldehyde, isoprene, and several aromatic compounds diluted with humid zero air. The response to formaldehyde was calibrated using a permeation device (KinTek).

The PTR-MS complemented the GC-MS-FID by providing more highly time-resolved VOC measurements. The GC-MS-FID had a low sampling frequency (maximum of one sample every seventy minutes), but was capable of quantifying individual monoterpene isomers for speciated analysis. The online GC-MS-FID was equipped with a custom-built automated sampling system, which is the same instrument described previously by Faiola et al.,[34] with two major improvements: cryo-trapping was replaced with Tenax GR adsorbent followed by thermodesorption, and an automated internal standard introduction system was added. Samples were

preconcentrated to detectable levels using Tenax GR adsorbent in a 1/8 in. diameter electropolished stainless steel tube. After 10 min of sampling, Tenax traps were heated to 300 °C to thermally desorb the analytes and transfer the sample to the GC column. The FID response (area nmol-C^{1-}) was calculated for each run with an internal standard, *n*-octane (Scott-Marin, 1.034 ppmV ± 2%). The internal standard was introduced to the sample flow using a mass flow controller (MFC, Alicat Scientific, model MC 100SCCM-D/5M) to dilute to 18 ppbV. Quantification was performed using the effective carbon numbers of the analytes giving a maximum instrumental error of ±10%.[34] Compounds were identified using a combination of monoterpene standard runs and mass spectra. Monoterpene standards were generated with a dynamic dilution system also described in detail by Faiola et al.[34]

The aerosol growth chamber dimensions were 1.6 × 2.2 × 2.2 m^3. Temperature and relative humidity were monitored with a Vaisala HMP110 humidity and temperature probe. Ozone was monitored with a dual beam ozone monitor (2B Technologies model 205B). Aerosol microphysical properties were measured with a scanning mobility particle sizer (SMPS, custom built with major components from TSI, Inc.). The recirculating sheath flow in the SMPS was set to 3 L min^{-1} and monodisperse aerosol flow was 0.3 L min^{-1}, so that the particle size range measured by the instrument was 20−730 nm. All volumes were corrected for wall loss using an established approach.[35,36] Two loss rate constants were determined using polydisperse ammonium sulfate particles generated with a constant output atomizer (TSI model 3076)—both with the aerosol chamber mixing fan on and with it off. With the mixing fan on, the loss rate constant was 0.0028 min^{-1} (r^2 = 0.99), which is consistent with those reported in the literature previously.[37] With the mixing fan off, particle loss was significantly reduced to a loss rate constant of 0.0005 min^{-1} (r^2 = 0.90). Thus, to promote mixing of VOCs and oxidant while reducing particle volume loss, the mixing fan was turned on during aerosol chamber loading and immediately turned off after oxidant addition.

For one experiment, aerosol composition was measured with a high resolution time-of-flight aerosol mass spectrometer (AMS, Aerodyne Research, Inc.).[38,39] The AMS was operated using v/w-mode switching with 30 s per save for each mode. An ionization efficiency calibration was performed the day prior to the experiment using the brute force single particle technique with 400 nm ammonium nitrate particles. A fragmentation table was used to generate chemically resolved information from unit mass resolution data.[40] Corrections were made to the fragmentation table to account for air fragmentation patterns at *m*/*z* 44, 29, 15, and 16. At the beginning and end of the chamber experiment, a high-efficiency particulate air (HEPA) filter was placed in the sampling line to collect filter runs, which were used to check the fragmentation modifications and to make further adjustments to correctly apportion the gas-phase signal. Only the unit mass resolution data from v-mode is presented here although high-resolution data was used to aid in fragmentation table corrections.

Experimental Procedure. The first set of samples collected on November 2, 2012 was used to conduct two proof-of-concept aerosol growth experiments—an initial investigation of the SOA formation potential of soil and litter VOC emissions. On the morning of each of these experiments, 1 L of tap water was added to each soil and litter pan to simulate a precipitation event because field measurements have shown bursts in emissions following rain.[21] The second set of samples, collected on November 9, 2012, was used to investigate baseline soil and litter emissions and SOA formation potential in more detail. These samples were allowed to dry naturally for 19 days, during which time five aerosol growth chamber experiments were performed. At the end of the second set of experiments, the recharge potential of the soil and litter was investigated by performing two additional precipitation simulation experiments 8 days apart from one another.

Preparations for each aerosol growth experiment began the day before, when the aerosol growth chamber was cleaned with 1 ppmV ozone (Enaly model HG-1500 ozone generator), and continuously purged overnight with zero air until ozone concentrations were less than 5 ppbV. On the day of the experiment, the aerosol growth chamber was switched from purging to batch mode. In batch mode, the aerosol chamber was loaded with soil and leaf litter VOC emissions from the soil emissions chamber for four hours using a chemically resistant vacuum pump (KNF Laboport model UN810 FTP). After loading the chamber, the oxidation of the emissions was initiated by rapidly adding ozone to the chamber; this defined the start of the experiment. Approximately 300 ppbV ozone was added to the first two proof-of-concept aerosol chamber experiments and 130 ppbV ozone was added to all other experiments. The aerosol chamber was not equipped with a UV light source and no hydroxyl radical scavenger was used, so the oxidative chemistry is best described as "dark ozone-initiated chemistry". No seed particles were added to the chamber. These idealized conditions resulted in the fast formation and growth of sufficient particles for our analysis. SOA microphysical and chemical properties were monitored during particle growth for 5−6 h after ozone addition.

RESULTS AND DISCUSSION

VOC Emission Rates: Temporal Patterns. A time series of the VOC emission rates from sample set 2 is shown in Figure 1. The VOC emission rate time series from sample set 1 is shown in SI Figure S2. Species measured by the GC-MS-FID are grouped by compound class and the sums of each class

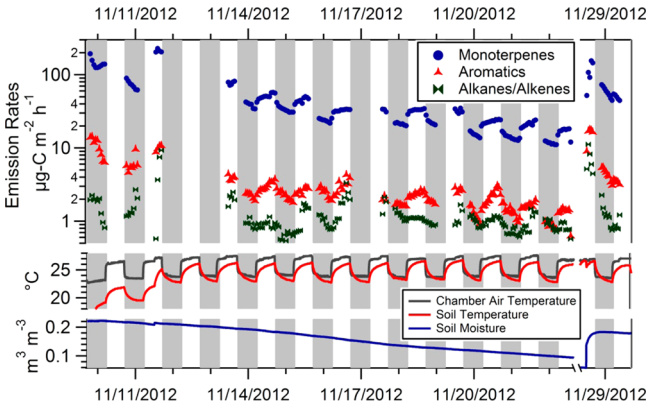

Figure 1. A time series of VOC emission rates from the second set of soil/litter samples. Emissions were dominated by monoterpenes (note log scale). Emissions were higher in the warmer daylight hours (unshaded) and decreased after the lamp was turned off (shaded gray). The overall trend was a decrease in emissions as the soil dried. Upon rewetting on November 28, 2012, emissions increased to nearly initial daytime levels. A second simulated precipitation event did not result in an emissions increase (not shown).

dx.doi.org/10.1021/es4040045 | Environ. Sci. Technol. 2014, 48, 938−946

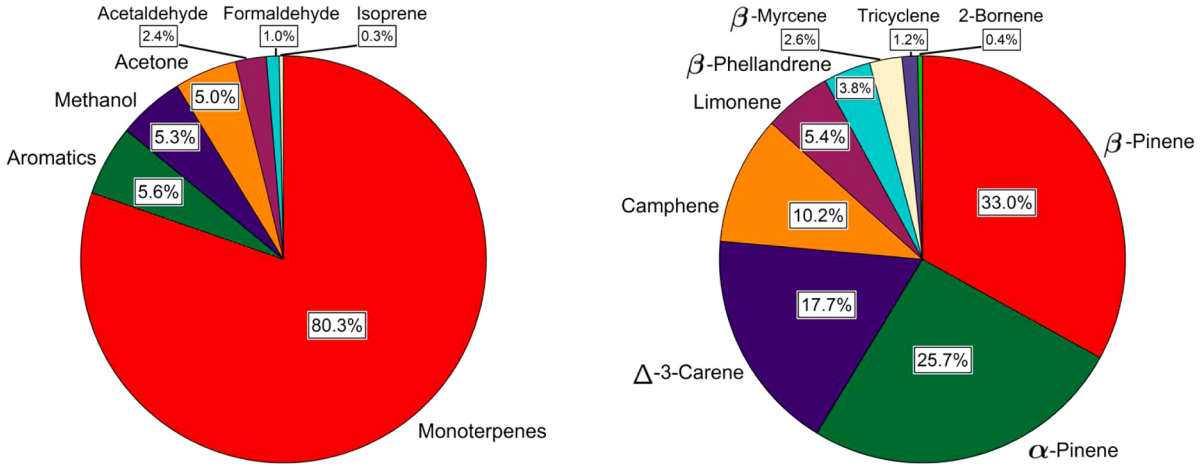

Figure 2. The VOC emission profile expressed on a relative carbon mass basis. The left figure illustrates the percentages of small oxygenated VOCs, aromatics, and terpenes as measured with the PTR-MS. Monoterpenes dominated the emission profile, comprising 80.3% of total VOC emissions shown. The right figure illustrates the speciated monoterpene emission profile measured with the GC-MS-FID. β-Pinene, α-pinene, Δ-3-carene, and camphene comprised greater than 85% of total monoterpene emissions. This monoterpene profile is consistent with litter composed of the dominant tree species at the sampling site—ponderosa pine and Douglas-fir.

(monoterpenes, aromatics, and alkanes/alkenes) are plotted in units of μg-C m^{-2} h^{-1} (carbon mass basis). Soil moisture, soil temperature, and air temperature are also shown. Alternate white and gray shading indicates the 12-h light/dark cycle. Emissions for each compound class started high as the samples warmed up in the lab after moving them from the field to the soil emissions chamber. The overall trend in emission rates decreased day-to-day as the soil began to dry. All compounds also demonstrated similar diel variabilities—emissions were higher during the warmer "daylight" hours (shaded white) and lower during the cooler "nighttime" hours (shaded gray). This pattern was more pronounced for the monoterpenes and aromatics than for the alkanes/alkenes, likely due to their differing saturation vapor pressures. The compounds included in the alkanes/alkenes group have higher vapor pressures and thus exhibit less temperature dependence in their emission rates. The maximum measured monoterpene emission rate was 228 μg-C m^{-2} h^{-1} (258 μg m^{-2} h^{-1} total). This rate was 2−3 orders of magnitude larger than the total litter monoterpene emissions of 0.1 μg m^{-2} h^{-1} and 5 μg m^{-2} h^{-1} reported by Greenberg et al.[21] and Aaltonen et al.,[27] respectively. The Greenberg et al.[21] measurements were performed in July, when it is possible the pool of terpenoid compounds in the litter has been depleted. Aaltonen et al.[27] made measurements from late April to November and noted that they observed a decreasing trend in emissions from April 28th to May 20th. They postulated that the emissions may have been even higher before their observations began in late April. This hypothesis is consistent with measurements made by Hellén et al.[29] at the same boreal forest site in Finland. They observed the highest emissions recorded at the site in early April. Our observations were consistent with these earlier results in Finland where peak total monoterpene emissions of 373 μg m^{-2} h^{-1} were observed immediately following snowmelt.

The final day shown in Figure 1 illustrates a rewetting event. In response to watering, emissions quickly increased to nearly the same values as the initial measurements (155 μg-C m^{-2} h^{-1}) and started to decrease again within 12 h. Emission bursts following precipitation events have previously been observed in field measurements.[21] The exact cause for the emission burst seen here could not be determined from the measurements. We hypothesize that it was likely due to an abiological phenomenon described previously by Warneke et al.[18] Briefly, under dry conditions, the nonpolar organic compounds adsorb to the soil and litter surfaces. The introduction of water molecules disrupts this interaction because the polar water molecules preferentially bind to the surfaces. The potential for a biological influence on emission rates has also been reported,[17] but is unlikely to be the controlling factor here—the emission burst was nearly instantaneous following rewetting and a biological influence related to microbial decomposition activity would not be expected on such a short time scale.

An additional rewetting was performed on December 6, 2012 (not shown). In this case, there was no observed increase in VOC emission rates. This suggests that the reservoir of VOCs available for release is limited (and depletable), and provides further evidence that the mechanism linking moisture to emissions is abiotic rather than due to microbial decomposition. If the latter mechanism were dominant, then it is unlikely that the pool of VOCs would deplete when heat, moisture, and litter were all still available. In any event, our results indicate clearly that more measurements are required before the processes leading to VOC emissions from litter can be reliably parametrized. Monoterpene emission rates from soil and litter may be primarily controlled by temperature, as they are for canopy emissions. However, the impact of other abiotic factors such as moisture, pH, exposure to freeze/thaw cycles, litter composition, and litter mass/depth should also be investigated in future work.

VOC Emission Rates: Chemical Profile. The percentages of small oxygenated VOCs, aromatics, isoprene, and monoterpene emissions measured with the PTR-MS are shown in Figure 2 on the left. The VOC profile was consistent throughout both sets of soil and litter samples with two exceptions: (1) higher variability in all emissions was observed the day after transporting the samples to the laboratory; and (2) there was an unexplained increase in acetaldehyde on November 19, 2012. The average percentages shown in Figure 2 were calculated from the average emission rates measured from November 7−17, 2012 and span both sets of samples. Monoterpenes dominated the average emission profile comprising 80.3% of the sum total carbon mass of the organic

dx.doi.org/10.1021/es4040045 | Environ. Sci. Technol. 2014, 48, 938−946

emissions shown. Aromatics made up 5.6% of total emissions. Based on GC-FID-MS analysis, aromatic emissions were dominated by toluene and cymenes with smaller amounts of acetophenone, isoprenyltoluene, and three unidentified aromatic components. The emission profile of the small oxygenated VOCs was dominated by methanol, comprising 5.3% of the total organic emissions. Acetone, acetaldehyde, and formaldehyde followed and were 5.0%, 2.4%, and 0.3% of total organic carbon mass emissions, respectively. This profile was consistent with previous measurements of litter emissions of small oxygenated VOCs.[17,18,21]

The percentage of speciated monoterpenes relative to the sum total of monoterpenes is shown in Figure 2 on the right. These values were calculated from the average emission rates measured with the GC-MS-FID from November 13−22, 2012. This time period was selected from the second set of samples because it includes the longest continuous set of GC-FID-MS measurements. Monoterpene emissions were dominated by β-pinene, α-pinene, Δ-3-carene, and camphene in descending order, which together account for more than 85% of the total monoterpene emissions. α-Fenchene was also identified, but was excluded from Figure 2 since it comprised less than 0.05% of the total. The monoterpene profile from the first set of samples was very similar (not shown). β-Pinene, α-pinene, Δ-3-carene, and camphene again comprised more than 85% of the total monoterpene emissions, but in this case, emissions of camphene were slightly greater than Δ-3-carene. This monoterpene emission profile was consistent with litter composed of a combination of ponderosa pine and Douglas fir needles—leaf litter extracts from both trees revealed terpene pools that were predominantly β-pinene for both trees followed by α-pinene for Douglas fir and Δ-3-carene for ponderosa pine.[41]

SOA Formation and Characteristics. A summary of all of the aerosol growth chamber experiments that were conducted using soil and litter emissions as the SOA precursor source is shown in Table 1. Experiments where the soil and litter samples were prewetted before the experiment to simulate a precipitation event are marked with an asterisk. The concentration of monoterpenes that reacted in the aerosol chamber was calculated by integrating GC-MS-FID measurements during VOC loading. Ozone was added in excess to ensure all monoterpenes reacted. This was confirmed by continuous sampling from the aerosol growth chamber with the PTR-MS—monoterpene concentrations quickly dropped to zero after ozone addition. Total particle volume was determined using the SMPS data.

Table 1. Summary Table of SOA Formation Experiments

experiment date	chamber experiment ID	soil moisture ($m^3\ m^{-3}$)	reacted monoterpenes ($\mu g\ m^{-3}$)	aerosol volume ($\mu m^3\ cm^{-3}$)
11/5/2012	1a	0.302[a]	242	5.43
11/8/2012	1b	0.507[a]	50	0.97
11/11/2012	2a	0.213	397	2.55
11/13/2012	2b	0.196	154	0.29
11/15/2012	2c	0.173	91	0.78
11/17/2012	2d	0.141	32	0.69
11/21/2012	2e	0.104	40	0.59
11/28/2012	2f	0.165[a]	201	4.32
12/6/2012	2g	0.223[a]	48	0.94

[a]Precipitation events were simulated by watering the soil and leaf litter prior to aerosol chamber loading.

Particle volume values shown in the experiment summary table are the maximum wall-loss corrected volumes that were observed in each experiment. The total aerosol volume generated was not consistently correlated with the monoterpene emission rates. A more comprehensive soil and litter SOA composition data set needs to be generated to determine whether or not the dominant SOA precursors are constant over time or if there are bursts in emissions not measured here that may contribute to variability. Amines have been suggested as potential aerosol precursors from soil and litter previously,[42,43] and would not have been detectable with the analytical equipment used here. Neither the PTR-MS nor the GC-MS-FID measured sesquiterpenes in significant amounts, but these compounds are known to have high losses in sampling lines[44,45] and previous work has indicated that aerosol yields can be very sensitive to the presence of sesquiterpenes.[46] Alternatively, inconsistencies in aerosol yield could be due to varying line losses for monoterpenes due to differences in humidity levels in the biogenic chamber. Such losses would have impacted the estimate of the concentration of monoterpenes that reacted.

If we assume that monoterpenes were the dominant SOA precursor and particle density was 1.4 g cm^{-3},[14] then the average aerosol yield was approximately 2.1%. The full range of estimated yields across all experiments was 0.3−3.1%. These values were consistent with previous lab studies; the dominant monoterpene emitted was β-pinene, which has an aerosol yield of 0−5%.[47] These results suggest that the SOA formation potential of leaf litter will depend on the vegetation type since different types of trees will store different terpenoids in their leaves or needles.

Particle composition was measured with an Aerodyne HR-ToF-AMS for one aerosol growth chamber experiment (December 6, 2012). The monoterpene profile that was loaded into the aerosol chamber for this experiment was consistent with the profile in Figure 2 and is shown in SI Figure S3. The organic unit mass resolution (UMR) spectrum is shown in Figure 3 along with two other UMR spectra for comparison: SOA generated from (1) ponderosa pine emissions and (2) α-pinene oxidation. α-Pinene oxidation was chosen for comparison because it has been the most studied of all single-component biogenic precursors and has long been used as a model compound for generalized biogenic SOA formation.[47] All spectra were normalized to the sum of the organic mass and are presented as a percent of the total organic mass. The reference AMS spectra from the dark ozonolysis of α-pinene was obtained from Bahreini et al.[48]

Scatter plots comparing the AMS UMR spectra to one another are also shown in Figure 3. For comparison purposes, m/z 28 and 18 were removed from the soil/litter and ponderosa pine SOA UMR spectra since they had been omitted from the reference α-pinene SOA spectra due to known complications attributing the appropriate fraction of these peaks to the organic aerosol component.[49,50] All three UMR organic spectra were similar with slopes between 0.95 and 1.09 and r^2 values ≥0.86 for all three comparisons (the comparisons included all m/z 12−195 except m/z 18 and 28). Of particular note, SOA generated from the soil/litter emissions and from live ponderosa pine were nearly identical (r^2 = 0.98, slope = 0.95). In a previous study, SOA generated from real plant emissions has been compared to reference α-pinene SOA with Pearson's correlation coefficients (R^2)

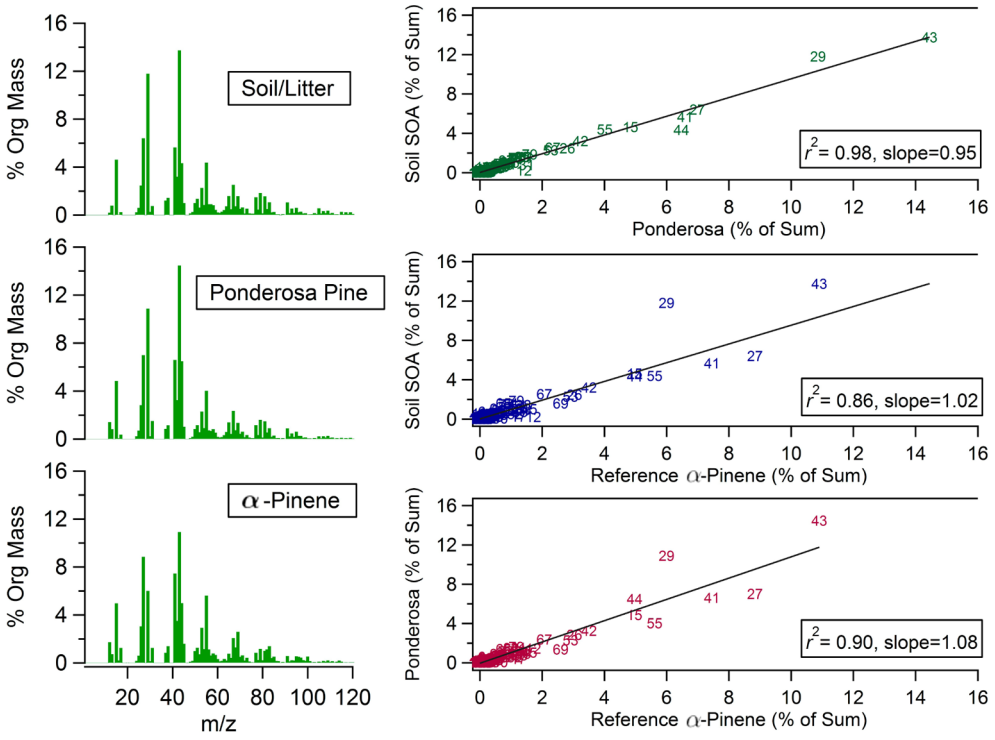

Figure 3. Composition of SOA generated from oxidation of various biogenic precursors: soil/litter emissions, ponderosa pine emissions, and α-pinene. The left side of the panel illustrates the organic UMR spectrum of each. UMR peaks were normalized to the sum of the organic signal. The α-pinene SOA spectrum was obtained from Bahreini et al.[48] The right side of the panel shows scatter plots comparing the different UMR spectra to one another. All three spectra were similar. Specifically, soil/litter SOA and ponderosa SOA were nearly identical with r^2 = 0.98.

ranging from 0.86 to 0.96.[51] The range in correlation coefficients represents correlations with six different biogenic SOA produced by different plants and/or under different temperature conditions. All biogenic SOA were well correlated with the average plant spectra with correlation coefficients ranging from 0.90 to 0.98. This strongly suggests that all freshly formed biogenic SOA from gas-phase oxidation can be modeled as a single type. Kiendler-Scharr et al.[51] further demonstrated that biogenic SOA formed from real plant emissions was significantly different from diesel exhaust organic aerosol (R^2 = 0.44−0.51), biomass burning organic aerosol (R^2 = 0.44−0.51), and hydrocarbon-like organic aerosol from Pittsburgh, PA (R^2 = 0.16−0.41).

Potential Contribution to Total Forest Emissions. To estimate the potential contribution of the soil and litter monoterpene emissions to total forest emissions, canopy monoterpene emission rates were modeled using MEGAN (v2.1beta).[16] Model input was selected based on reasonable values for comparison with measurements. Input meteorological values reflected fall and spring conditions at the sampling site—a time of year when leaf litter has the potential to significantly contribute to the total forest emissions. The model input temperature data were obtained from the weather station at the nearby Plummer, ID airport for March and April 2013 and from the nearby Moscow, ID weather station for November 2012. Solar radiation was determined using the NCAR TUV calculator for the latitude, longitude, and altitude of the sampling site.[52] Emission Type 1 (ET1) was used to define the vegetation, which describes needleleaf evergreen temperate trees similar to the vegetation at the sampling site. The default leaf area index of five was used, which is reasonable for a temperate coniferous forest such as this.[53,54] Monoterpene emissions were temperature-normalized to 30 °C for comparison using a value of 0.09 for the activity adjustment factor (β).[55] A temperature condition of 30 °C was chosen as has been recommended for reporting "basal emission" rates of monoterpene emissions from vegetation.[56] The average modeled monoterpene emission rate for the first week in November was 229 $\mu g\ m^{-2}\ h^{-1}$ ± 6% and for the first week of March was 231 $\mu g\ m^{-2}\ h^{-1}$ ± 5%. Since the monoterpene source in MEGAN is live tree emissions, these average modeled emission rates were used to estimate the fall and spring canopy monoterpene emission rates, respectively.

The laboratory measurements of soil and litter monoterpene emission rates were split into four categories for comparison with model results: initial daytime, drying, minimum, and rewet spike. The values for these categories were calculated as follows: "initial daytime" is the average of the first daytime measurements on November 11, 2012 after moving the soil sample to the laboratory; "drying" is the average value from November 13−14, 2012; "minimum" is the average from November 21−22, 2012; and "re-wet spike" is the average of the two maximum points after the soil and litter was watered to simulate a precipitation event on November 28, 2012. This approach to data analysis was used in order to investigate the potential range of the surface contribution (soil and litter) to total forest monoterpene emission rate.

The monoterpene emission rates of the surface (measured) and the canopy (estimated) are shown in Figure 4. Error bars were calculated from the relative standard deviation of the averaged emission rate values. The highest surface emissions were observed for initial daytime measurements—surface emissions were 34−36% higher than the estimated canopy emissions. The lowest surface emissions were observed after the

dx.doi.org/10.1021/es4040045 | Environ. Sci. Technol. 2014, 48, 938−946

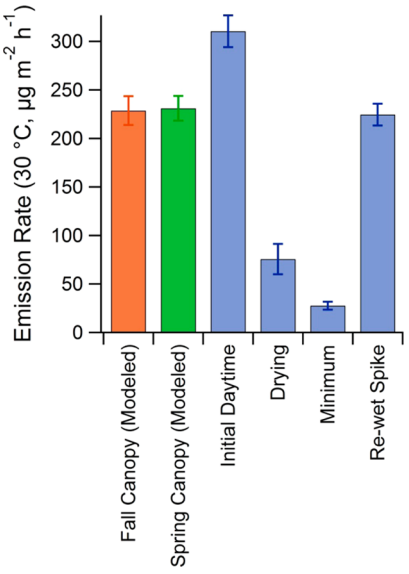

Figure 4. Potential range of surface monoterpene emission rates compared to modeled canopy monoterpene emission rates from fall and spring. All emissions were normalized to a temperature of 30 °C for comparison. The highest surface emissions were observed during the initial daytime measurements when surface emissions were 34–36% higher than modeled canopy emissions. The minimum surface emissions were 12% of canopy emissions. A simulated precipitation event increased emissions to approximately the same value as canopy emissions (97–98%).

samples had been in the lab for 12 days and had dried out substantially; even then, surface emissions were 12% of the modeled canopy monoterpene emission rates. After rewetting the soil, the surface contribution increased to approximately the same value as the canopy (97–98% of the modeled canopy emission values), but the spike was short-lived and came back down to initial drying levels within 24 h. Drying surface emissions were 33% of the estimated canopy emissions.

On the basis of these estimates, surface monoterpene emissions in spring and fall could range from 12–136% of canopy emissions. These results suggest a significant portion of total forest monoterpene emission rates could be controlled by factors that affect soil and litter emissions rather than factors that affect plant emissions—factors that have remained unexplored so far. A clear impact of such emissions would be on regional organic aerosol and ozone formation. As demonstrated with aerosol chamber experiments, SOA was formed from leaf litter emissions, and the organic composition was very similar to aerosol formed from whole plant emissions from ponderosa pine. Emissions from leaf litter may potentially extend the biogenic emissions season, contributing to significant organic aerosol formation in the spring and fall when reduced PAR and temperatures reduce emission rates from vegetation.

■ ASSOCIATED CONTENT

Supporting Information

Dual chamber system schematic (Figure S1); VOC time series of soil sample set 1 ("proof-of-concept experiments") (Figure S2); and the monoterpene profile while the chamber was being loaded for the experiment and the included AMS composition measurements (Figure S3). This material is available free of charge via the Internet at http://pubs.acs.org.

■ AUTHOR INFORMATION

Corresponding Author

*Phone: 509-335-5055; fax: 509-335-7632; e-mail: vanreken@wsu.edu.

Notes

The authors declare no competing financial interest.

■ ACKNOWLEDGMENTS

The authors thank Brian Austin of the University of Idaho Experimental Forest for his assistance during the sample collection, Alex Guenther and Tsengel Nergui for advice on using the MEGAN model, and Kara Yedinak for her support and encouragement. This work was supported by the U.S. Department of Energy Early Career Research Program (Award No. SC0003899).

■ REFERENCES

(1) Jimenez, J. L.; Canagaratna, M. R.; Donahue, N. M.; Prevot, A. S. H.; Zhang, Q.; Kroll, J. H.; DeCarlo, P. F.; Allan, J. D.; Coe, H.; Ng, N. L.; Aiken, A. C.; Docherty, K. S.; Ulbrich, I. M.; Grieshop, A. P.; Robinson, A. L.; Duplissy, J.; Smith, J. D.; Wilson, K. R.; Lanz, V. A.; Hueglin, C.; Sun, Y. L.; Tian, J.; Laaksonen, A.; Raatikainen, T.; Rautiainen, J.; Vaattovaara, P.; Ehn, M.; Kulmala, M.; Tomlinson, J. M.; Collins, D. R.; Cubison, M. J.; Dunlea, J.; Huffman, J. A.; Onasch, T. B.; Alfarra, M. R.; Williams, P. I.; Bower, K.; Kondo, Y.; Schneider, J.; Drewnick, F.; Borrmann, S.; Weimer, S.; Demerjian, K.; Salcedo, D.; Cottrell, L.; Griffin, R.; Takami, A.; Miyoshi, T.; Hatakeyama, S.; Shimono, A.; Sun, J. Y.; Zhang, Y. M.; Dzepina, K.; Kimmel, J. R.; Sueper, D.; Jayne, J. T.; Herndon, S. C.; Trimborn, A. M.; Williams, L. R.; Wood, E. C.; Middlebrook, A. M.; Kolb, C. E.; Baltensperger, U.; Worsnop, D. R. Evolution of organic aerosols in the atmosphere. *Science* **2009**, *326*, 1525–1529.

(2) Zhang, Q.; Jimenez, J. L.; Canagaratna, M. R.; Allan, J. D.; Coe, H.; Ulbrich, I.; Alfarra, M. R.; Takami, A.; Middlebrook, A. M.; Sun, Y. L.; Dzepina, K.; Dunlea, E.; Docherty, K.; DeCarlo, P. F.; Salcedo, D.; Onasch, T.; Jayne, J. T.; Miyoshi, T.; Shimono, A.; Hatakeyama, S.; Takegawa, N.; Kondo, Y.; Schneider, J.; Drewnick, F.; Borrmann, S.; Weimer, S.; Demerjian, K.; Williams, P.; Bower, K.; Bahreini, R.; Cottrell, L.; Griffin, R. J.; Rautiainen, J.; Sun, J. Y.; Zhang, Y. M.; Worsnop, D. R. Ubiquity and dominance of oxygenated species in organic aerosols in anthropogenically-influenced northern hemisphere midlatitudes. *Geophys. Res. Lett.* **2007**, *34*, L13801.

(3) Prenni, A. J.; DeMott, P. J.; Kreidenweis, S. M. Water uptake of internally mixed particles containing ammonium sulfate and dicarboxylic acids. *Atmos. Environ.* **2003**, *37*, 4243–4251.

(4) Raymond, T. M.; Pandis, S. N. Cloud activation of single-component organic aerosol particles. *J. Geophys. Res. Atmos.* **2002**, *107*, 4787.

(5) Forster, P.; Ramaswamy, V.; Artaxo, P.; Berntsen, T.; Betts, R.; Fahey, D.W.; Haywood, J.; Lean, J.; Lowe, D.C.; Myhre, G.; Nganga, J.; Prinn, R.; Raga, G.; Schulz, M.; Van Dorland, R. *Climate Change 2007: The Physical Science Basis. Contribution of Working Group I to the Fourth Assessment Report of the Intergovernmental Panel on Climate Change*; Cambridge University Press: Cambridge, UK and New York, USA, 2007.

(6) Dzepina, K.; Volkamer, R. M.; Madronich, S.; Tulet, P.; Ulbrich, I. M.; Zhang, Q.; Cappa, C. D.; Ziemann, P. J.; Jimenez, J. L. Evaluation of recently-proposed secondary organic aerosol models for a case study in Mexico City. *Atmos. Chem. Phys.* **2009**, *9*, 5681–5709.

(7) Heald, C. L.; Coe, H.; Jimenez, J. L.; Weber, R. J.; Bahreini, R.; Middlebrook, A. M.; Russell, L. M.; Jolleys, M.; Fu, T.-M.; Allan, J. D.; Bower, K. N.; Capes, G.; Crosier, J.; Morgan, W. T.; Robinson, N. H.; Williams, P. I.; Cubison, M. J.; DeCarlo, P. F.; Dunlea, E. J. Exploring the vertical profile of atmospheric organic aerosol: Comparing 17 aircraft field campaigns with a global model. *Atmos. Chem. Phys.* **2011**, *11*, 12673–12696.

(8) Spracklen, D. V.; Jimenez, J. L.; Carslaw, K. S.; Worsnop, D. R.; Evans, M. J.; Mann, G. W.; Zhang, Q.; Canagaratna, M. R.; Allan, J.; Coe, H.; McFiggans, G.; Rap, A.; Forster, P. Aerosol mass spectrometer constraint on the global secondary organic aerosol budget. *Atmos. Chem. Phys.* **2011**, *11*, 12109−12136.
(9) Volkamer, R.; Jimenez, J. L.; San Martini, F.; Dzepina, K.; Zhang, Q.; Salcedo, D.; Molina, L. T.; Worsnop, D. R.; Molina, M. J. Secondary organic aerosol formation from anthropogenic air pollution: Rapid and higher than expected. *Geophys. Res. Lett.* **2006**, *33*, L17811.
(10) Atkinson, R. Atmospheric chemistry of VOCs and NOx. *Atmos. Environ.* **2000**, *34*, 2063−2101.
(11) Kroll, J. H.; Seinfeld, J. H. Chemistry of secondary organic aerosol: Formation and evolution of low-volatility organics in the atmosphere. *Atmos. Environ.* **2008**, *42*, 3593−3624.
(12) Carlton, A. G.; Pinder, R. W.; Bhave, P. V.; Pouliot, G. A. To what extent can biogenic SOA be controlled? *Environ. Sci. Technol.* **2010**, *44*, 3376−3380.
(13) Hoyle, C. R.; Boy, M.; Donahue, N. M.; Fry, J. L.; Glasius, M.; Guenther, A.; Hallar, A. G.; Huff Hartz, K.; Petters, M. D.; Petäjä, T.; Rosenoern, T.; Sullivan, A. P. A review of the anthropogenic influence on biogenic secondary organic aerosol. *Atmos. Chem. Phys.* **2011**, *11*, 321−343.
(14) Hallquist, M.; Wenger, J. C.; Baltensperger, U.; Rudich, Y.; Simpson, D.; Claeys, M.; Dommen, J.; Donahue, N. M.; George, C.; Goldstein, A. H.; Hamilton, J. F.; Herrmann, H.; Hoffmann, T.; Iinuma, Y.; Jang, M.; Jenkin, M. E.; Jimenez, J. L.; Kiendler-Scharr, A.; Maenhaut, W.; McFiggans, G.; Mentel, T. F.; Monod, A.; Prévôt, A. S. H.; Seinfeld, J. H.; Surratt, J. D.; Szmigielski, R.; Wildt, J. The formation, properties and impact of secondary organic aerosol: Current and emerging issues. *Atmos. Chem. Phys.* **2009**, *9*, 5155−5235.
(15) Guenther, A.; Karl, T.; Harley, P.; Wiedinmyer, C.; Palmer, P. I.; Geron, C. Estimates of global terrestrial isoprene emissions using MEGAN (model of emissions of gases and aerosols from nature). *Atmos. Chem. Phys.* **2006**, *6*, 3181−3210.
(16) Guenther, A. B.; Jiang, X.; Heald, C. L.; Sakulyanontvittaya, T.; Duhl, T.; Emmons, L. K.; Wang, X. The model of emissions of gases and aerosols from nature version 2.1 (MEGAN2.1): An extended and updated framework for modeling biogenic emissions. *Geosci. Model. Dev.* **2012**, *5*, 1471−1492.
(17) Gray, C. M.; Monson, R. K.; Fierer, N. Emissions of volatile organic compounds during the decomposition of plant litter. *J. Geophys. Res. Biogeosci.* **2010**, *115*, 10.1029/2010JG001291.
(18) Warneke, C.; Karl, T.; Judmaier, H.; Hansel, A.; Jordan, A.; Lindinger, W.; Crutzen, P. J. Acetone, methanol, and other partially oxidized volatile organic emissions from dead plant matter by abiological processes: Significance for atmospheric HOx chemistry. *Glob. Biogeochem. Cycles* **1999**, *13*, 9−17.
(19) Isidorov, V. A.; Vinogorova, V. T.; Rafalowski, K. HS-SPME analysis of volatile organic compounds of coniferous needle litter. *Atmos. Environ.* **2003**, *37*, 4645−4650.
(20) Isidorov, V.; Jdanova, M. Volatile organic compounds from leaves litter. *Chemosphere* **2002**, *48*, 975−979.
(21) Greenberg, J. P.; Asensio, D.; Turnipseed, A.; Guenther, A. B.; Karl, T.; Gochis, D. Contribution of leaf and needle litter to whole ecosystem BVOC fluxes. *Atmos. Environ.* **2012**, *59*, 302−311.
(22) Hayward, S.; Muncey, R. .; James, A. .; Halsall, C. .; Hewitt, C. Monoterpene emissions from soil in a Sitka spruce forest. *Atmos. Environ.* **2001**, *35*, 4081−4087.
(23) Janson, R. W. Monoterpene emissions from Scots Pine and Norwegian Spruce. *J. Geophys. Res. Atmos.* **1993**, *98*, 2839−2850.
(24) Janson, R.; De Serves, C.; Romero, R. Emission of isoprene and carbonyl compounds from a boreal forest and wetland in Sweden. *Agric. For. Meteorol.* **1999**, *98*, 671−681.
(25) Mäkelä, J. M.; Maso, M. D.; Pirjola, L.; Keronen, P.; Laakso, L.; Kulmala, M.; Laaksonen, A. Characteristics of the atmospheric particle formation events observed at a borel forest site in southern Finland. *Boreal Environ. Res.* **2000**, *5*, 299−313.
(26) Bigg, E. K. Gas emissions from soil and leaf litter as a source of new particle formation. *Atmos. Res.* **2004**, *70*, 33−42.
(27) Aaltonen, H.; Pumpanen, J.; Pihlatie, M.; Hakola, H.; Hellén, H.; Kulmala, L.; Vesala, T.; Bäck, J. Boreal pine forest floor biogenic volatile organic compound emissions peak in early summer and autumn. *Agric. For. Meteorol.* **2011**, *151*, 682−691.
(28) Isidorov, V. A.; Smolewska, M.; Purzynska-Pugacewicz, A.; Tyszkiewicz, Z. Chemical composition of volatile and extractive compounds of pine and spruce leaf litter in the initial stages of decomposition. *Biogeosciences* **2010**, *7*, 2785−2794.
(29) Hellén, H.; Hakola, H.; Pystynen, K.-H.; Rinne, J.; Haapanala, S. C2−C10 hydrocarbon emissions from a boreal wetland and forest floor. *Biogeosciences* **2006**, *3*, 167−174.
(30) Sparks, D. L. *Methods of Soil Analysis. Part 3. Chemical Methods*; Sparks, D. L., Ed.; American Society of Agronomy-Soil Science Society of America, 1996.
(31) National Resource Conservation Service Web Soil Survey, http://websoilsurvey.sc.egov.usda.gov/App/HomePage.htm.
(32) Lindinger, W.; Hansel, A.; Jordan, A. On-line monitoring of volatile organic compounds at pptv levels by means of proton-transfer-reaction mass spectrometry (PTR-MS) medical applications, food control and environmental research. *Int. J. Mass Spectrom. Ion Process.* **1998**, *173*, 191−241.
(33) Jobson, B. T.; McCoskey, J. K. Sample drying to improve HCHO measurements by PTR-MS instruments: Laboratory and field measurements. *Atmos. Chem. Phys.* **2010**, *10*, 1821−1835.
(34) Faiola, C. L.; Erickson, M. H.; Fricaud, V. L.; Jobson, B. T.; VanReken, T. M. Quantification of biogenic volatile organic compounds with a flame ionization detector using the effective carbon number concept. *Atmos. Meas. Tech.* **2012**, *5*, 1911−1923.
(35) Pathak, R. K.; Stanier, C. O.; Donahue, N. M.; Pandis, S. N. Ozonolysis of α-pinene at atmospherically relevant concentrations: Temperature dependence of aerosol mass fractions (yields). *J. Geophys. Res. Atmos.* **2007**, *112*, 10.1029/2006JD007436.
(36) Presto, A. A.; Donahue, N. M. Investigation of α-pinene + ozone secondary organic aerosol formation at low total aerosol mass. *Environ. Sci. Technol.* **2006**, *40*, 3536−3543.
(37) Hao, L. Q.; Romakkaniemi, S.; Yli-Pirilä, P.; Joutsensaari, J.; Kortelainen, A.; Kroll, J. H.; Miettinen, P.; Vaattovaara, P.; Tiitta, P.; Jaatinen, A.; Kajos, M. K.; Holopainen, J. K.; Heijari, J.; Rinne, J.; Kulmala, M.; Worsnop, D. R.; Smith, J. N.; Laaksonen, A. Mass yields of secondary organic aerosols from the oxidation of α-pinene and real plant emissions. *Atmos. Chem. Phys.* **2011**, *11*, 1367−1378.
(38) Canagaratna, M. R.; Jayne, J. T.; Jimenez, J. L.; Allan, J. D.; Alfarra, M. R.; Zhang, Q.; Onasch, T. B.; Drewnick, F.; Coe, H.; Middlebrook, A.; Delia, A.; Williams, L. R.; Trimborn, A. M.; Northway, M. J.; DeCarlo, P. F.; Kolb, C. E.; Davidovits, P.; Worsnop, D. R. Chemical and Microphysical Characterization of Ambient Aerosols with the Aerodyne Aerosol Mass Spectrometer. *Mass Spectrom. Rev.* **2007**, *26*, 185−222.
(39) DeCarlo, P. F.; Kimmel, J. R.; Trimborn, A.; Northway, M. J.; Jayne, J. T.; Aiken, A. C.; Gonin, M.; Fuhrer, K.; Horvath, T.; Docherty, K. S.; Worsnop, D. R.; Jimenez, J. L. Field-deployable, high-resolution, time-of-flight aerosol mass spectrometer. *Anal. Chem.* **2006**, *78*, 8281−8289.
(40) Allan, J. D.; Delia, A. E.; Coe, H.; Bower, K. N.; Alfarra, M. R.; Jimenez, J. L.; Middlebrook, A. M.; Drewnick, F.; Onasch, T. B.; Canagaratna, M. R. A generalised method for the extraction of chemically resolved mass spectra from aerodyne aerosol mass spectrometer data. *J. Aerosol Sci.* **2004**, *35*, 909−922.
(41) Geron, C.; Rasmussen, R.; R Arnts, R.; Guenther, A. A review and synthesis of monoterpene speciation from forests in the United States. *Atmos. Environ.* **2000**, *34*, 1761−1781.
(42) Mäkelä, J. M.; Yli-Koivisto, S.; Hiltunen, V.; Seidl, W.; Swietlicki, E.; Teinilä, K.; Sillanpää, M.; Koponen, I. K.; Paatero, J.; Rosman, K.; Hämeri, K. Chemical composition of aerosol during particle formation events in boreal forest. *Tellus B* **2001**, *53*, 380−393.
(43) Smith, J. N.; Barsanti, K. C.; Friedli, H. R.; Ehn, M.; Kulmala, M.; Collins, D. R.; Scheckman, J. H.; Williams, B. J.; McMurry, P. H. Observations of aminium salts in atmospheric nanoparticles and

possible climatic implications. *Proc. Natl. Acad. Sci.* **2010**, *107*, 6634−6639.
(44) Helmig, D.; Bocquet, F.; Pollmann, J.; Revermann, T. Analytical techniques for sesquiterpene emission rate studies in vegetation enclosure experiments. *Atmos. Environ.* **2004**, *38*, 557−572.
(45) Helmig, D.; Ortega, J.; Duhl, T.; Tanner, D.; Guenther, A.; Harley, P.; Wiedinmyer, C.; Milford, J.; Sakulyanontvittaya, T. Sesquiterpene emissions from pine trees—Identifications, emission rates and flux estimates for the contiguous United States. *Environ. Sci. Technol.* **2007**, *41*, 1545−1553.
(46) VanReken, T.; Greenberg, J.; Harley, P.; Guenther, A.; Smith, J. Direct measurement of particle formation and growth from the oxidation of biogenic emissions. *Atmos. Chem. Phys.* **2006**, *6*, 4403−4413.
(47) Griffin, R. J.; Cocker, D. R.; Flagan, R. C.; Seinfeld, J. H. Organic aerosol formation from the oxidation of biogenic hydrocarbons. *J. Geophys. Res. Atmos.* **1999**, *104*, 3555−3567.
(48) Bahreini, R.; Keywood, M. D.; Ng, N. L.; Varutbangkul, V.; Gao, S.; Flagan, R. C.; Seinfeld, J. H.; Worsnop, D. R.; Jimenez, J. L. Measurements of secondary organic aerosol from oxidation of cycloalkenes, terpenes, and *m*-xylene using an aerodyne aerosol mass spectrometer. *Environ. Sci. Technol.* **2005**, *39*, 5674−5688.
(49) Allan, J. D.; Jimenez, J. L.; Williams, P. I.; Alfarra, M. R.; Bower, K. N.; Jayne, J. T.; Coe, H.; Worsnop, D. R. Quantitative sampling using an aerodyne aerosol mass spectrometer 1. Techniques of data interpretation and error analysis. *J. Geophys. Res. Atmos.* **2003**, *108*, 10.1029/2002JD002358.
(50) Zhang, Q.; Worsnop, D. R.; Canagaratna, M. R.; Jimenez, J. L. Hydrocarbon-like and oxygenated organic aerosols in Pittsburgh: Insights into sources and processes of organic aerosols. *Atmos. Chem. Phys.* **2005**, *5*, 3289−3311.
(51) Kiendler-Scharr, A.; Zhang, Q.; Hohaus, T.; Kleist, E.; Mensah, A.; Mentel, T. F.; Spindler, C.; Uerlings, R.; Tillmann, R.; Wildt, J. Aerosol mass spectrometric features of biogenic SOA: Observations from a plant chamber and in rural atmospheric environments. *Environ. Sci. Technol.* **2009**, *43*, 8166−8172.
(52) NCAR Quick TUV Calculator, http://cprm.acd.ucar.edu/Models/TUV/Interactive_TUV/.
(53) Soudani, K.; Francois, C.; Le Maire, G.; Le Dantec, V.; Dufrêne, E. Comparative analysis of IKONOS, SPOT, and ETM+ data for leaf area index estimation in temperate coniferous and deciduous forest stands. *Remote Sens. Environ.* **2006**, *102*, 161−175.
(54) Wang, Y.; Woodcock, C. E.; Buermann, W.; Stenberg, P.; Voipio, P.; Smolander, H.; Häme, T.; Tian, Y.; Hu, J.; Knyazikhin, Y. Evaluation of the MODIS LAI algorithm at a coniferous forest site in Finland. *Remote Sens. Environ.* **2004**, *91*, 114−127.
(55) Guenther, A.; Hewitt, C. N.; Erickson, D.; Fall, R.; Geron, C.; Graedel, T.; Harley, P.; Klinger, L.; Lerdau, M.; McKay, W. A.; et al. A global model of natural volatile organic compound emissions. *J. Geophys. Res. Atmos.* **1995**, *100*, 8873−8892.
(56) Ortega, J.; Helmig, D. Approaches for quantifying reactive and low-volatility biogenic organic compound emissions by vegetation enclosure techniques—Part A. *Chemosphere* **2008**, *72*, 343−364.